Deep Layered Network Model to Classify Brain Tumor in MRI Images

Saran Raj S. , S. V. Sudha, K. Padmanaban, P. Sherubha, S. P. Sasirekha
[1]Department of Computer Science andEngineering, Vel Tech Rangarajan Dr. Sagunthala R&D Institute of Science and Technology, Avadi, Chennai, India
[2]Professor, Department of Artificial Intelligence and Data Science, KPR Institute of Engineering and Technology, Coimbatore, India
[3]Department of Computer Science and Engineering, Koneru Lakshmaiah Education Foundation, Vaddeswaran, Guntur, Andhra Pradesh, India
[4]Assistant Professor, Department of Information Technology, Karpagam College of Engineering, Coimbatore, India
[5]Associate Professor, Department of Computer science and Engineering, Karpagam Academy of Higher Education, Coimbatore, India

Emails: sarandilip.er@gmail.com; sudha.sv@kpriet.ac.in; padmanaban.k@yahoo.com; sherubha0106@gmail.com; sugi.sasi29@yahoo.com

Abstract

Brain tumor is a condition due to the expansion of abnormal cell growth. Tumors are rare and can take many forms; it is challenging to estimate the survival rate of a patient. These tumors are found using Magnetic Resonance (MRI) which is crucial for locating the tumor region. Moreover, manual identification is an extensive and difficult method to produce false positives. The research communities have adopted computer-aided methods to overcome these limitations. With the advancement of artificial intelligence (AI), brain tumor prediction relies on MR images and deep learning (DL) models in medical imaging. The suggested layered configurations, i.e., layered network model, are proposed to classify and detect brain tumors accurately. The modified CNN is proposed to automatically detect the important features without any supervision and the convolution layer present in the network model enhances the training feasibility. To improve the quality of the images, some essential pre-processing is used in conjunction with image-enhancing methods. Data augmentation is adopted to expand the number of data samples for our suggested model's training. The Dataset is portioned as based on 70% for training and 30% for testing. The findings demonstrate that the proposed model works well than existing models in classification **precision**, accuracy, **recall, and area under the curve**. The layered network model beats other CNN models and achieves an overall accuracy of 99% during prediction. In addition, VGG16, hybrid CNN and NADE, CNN, CNN and KELM, deep CNN with data augmentation, CNN-GA, hybrid VGG16-NADE and ResNet+SE approaches are used for comparison.

Keywords: brain tumor; deep learning; layered network model; prediction accuracy and pre-processing.

1. Introduction

Brain tumor is a condition encountered with the growth of aberrant brain tissues or cells. Typically, cells replace one another as they divide and die in a predictable order. However, some cells develop abnormally and multiply, severely impairing brain activity and frequently resulting in death [1]. There are at least 120 different kinds of brain tumors and CNS disorders. In 2021, brain and CNS cancers will cause 18,600 adult deaths and 3,460 deaths in children under 15. Only 36% of individuals with brain tumors survive for five years, and only 31% survive for ten. In 2019, 86,010 new CNS and multiple brain cancers were found in the US, according to the report of the National Cancer Institute [2]. According to estimates, 0.7 million individuals today have brain tumors. There were 0.86 million documented cases, with 26,170 patients having malignant tumors and 60,800 patients having benign tumors. According to the WHO, 10 million people were given cancer diagnoses in 2019 [3].Early brain tumor identification is among the key factors in saving a patient's life. To assess a patient's status, it is essential to

Doi : https://doi.org/10.54216/JCIM.140202
Received: January 19, 2024 Revised: March 01, 2024 Accepted: June 07, 2024

examine brain tumor images properly. MRIisanalyzed for predicting anomalies and choices are made by a physician or radiologist as part of the traditional procedure for finding brain cancers [4]. However, it heavily depends on a doctor's medical knowledge; variations in experimental levels and the images nature makes diagnosesmore difficult. Given that they have several irregularities or noisy data, these images are difficult for a doctor to assess quickly [5]. Assessing a large amount of information becomes more difficult as the volume rises. A brain tumor's manual identification becomes increasingly time- and money-consuming. To save priceless human lives, an autonomous computer-aided diagnostic (CAD) system is needed to help radiologists and physicians identify these dangerous malignancies early [6].

Researchers are working to develop artificial intelligence (AI), which will enable machines to think, learn, and solve problems when presented with new knowledge [7]. To diagnose brain cancers, AI is crucial. Due to its intricate and complex procedures, the field of brain tumor prediction is a great opportunity byenhancing AI model. There have been numerous attempts to develop a classification method for brain tumors that is incredibly exact and trustworthy [8]. The great variety of However, differences in shape, texture, and contrast within and across individuals continue to be a difficult issue to solve. The way neurosurgical procedures are carried out has radically changed due to recent developments in AI's Deep machine learning and education. Along with data preparation, they also discuss feature extraction, selection, reduction and categorization [9]. Neuro-surgeons are less in demand because AI is now less likely to diagnose a patient's brain tumor with greater certainty as they leave the operating room [10].

When deep learning produces promising outcomes, particularly neural networks, it becomes significantly more important. The extraordinary abilities of convolutional neural networks (CNNs) can learn features and offer limitless precision [11]. Numerous deep learning applications, such as those for pattern classification, are now decision-making processes for voice recognition, object identification, and other applications. Both traditional ML methods like Naive Bayes, k-nearest neighbor (k-NN), Decision trees, support vector machines (SVMs) and DLincluding customized CNNs, VGGNets, GoogleNets, and ResNets, have previously been utilized in studies are employed to aid the medical community in the diagnosis of such harmful diseases [12]. Despite several attempts by researchers to identify cancers using MRI scans, there are still major areas for improvement (i.e., poor precision, large, slow models, and expensive computation) [13]. More in-depth data continues to be a problem in the healthcare sector, as researchers are reluctant to discuss medical data publicly due to patient privacy concerns [14]. Additionally, because existing approaches have poorer precision and memory levels, they are less effective, take longer to categorize images, and may cause a delay in the patient's therapy [15].

Recent studies adopted deep learning (DL) to increase the efficiency of brain cancer research using computer-aided medical diagnostics. They are essential to the healthcare sector and are useful instruments for treating various serious ailments, including detecting brain diseases and interpreting skin cancer images. Depending on transfer learning, DL techniques are encouraged to fine-tune for categorizing brain tumors. Deep layered network modelis extensively tested in this study to automate the classification, diagnosis, and fine-tuning of brain tumors through machine learning. Our proposed study's main contributions are:

• Using our suggested layers, a revolutionary automated technique that uses a DL approach for brain tumor classification enhances the traditional CNN model, increasing classification accuracy overall.

• To improve results on small datasets, the data pre-processing technique is applied to resolve how over-fitting phenomena affect classification.

• A preliminary image processing step improves the MRI images' visual quality.

• Our suggested model is compared to various deep CNNs models employed in this work regarding the accuracy, weight sizes, and other factors. In every way, the suggested model performed better than the other CNNs.

The remaining sections of the essay are separated and structured: Some existing approaches are discussed in section 2. The proposed methodology shows the implementation details in Section 3, and the experimental findings of the suggested techniques are described in Section 4. Furthermore, the conclusion and recommendations for additional research are included in Section 5.

2. Related works

This section discusses several related research that consider conventional images in identifying and classifying viral brain tumors using DL approaches. Sangeetha et al. [16] have out a thorough investigation into various brain

Doi : https://doi.org/10.54216/JCIM.140202
Received: January 19, 2024 Revised: March 01, 2024 Accepted: June 07, 2024

MRI image diagnostic techniques. Additionally, the authors examined the performance indicators and constraints of both traditional DL techniques. The authors of [17] discussed several methods for identifying brain tumors from MR images. Their research used multi-class SVMs, CNNs, and three-dimensional SVMs for segmentation in depth. Compared to other ML classifiers, the DL methodology delivered excellent results and a reliable segmentation and classification method for brain tumors.

To haul out the characteristics from the MRI and supply them as input to ML classifiers, the authors of a previous study presented a deep learning neural model (Naive Bayes, SVMs, and Multilayer perceptron) [18]. With SVMs as the classifiers, the suggested technique achieved 96% classification accuracy. For brain tumor classification, Dogo et al. [19] offered several machines and DL techniques, including approaches using Naive Bayes, SVMs, K-NN, multi-layer perceptrons, and random forests. Traditional SVMs could categorize data with the highest accuracy (92.4%) of all these techniques. They also suggested a five-layer customized CNN design that, when used to identify brain tumors in MR images, had a detection rate of 97.2%. Wei et al. [20] investigated brain tumor classification and segmentation was proposed using a combination of K-means clustering and VGG19 CNN architecture. The suggested approach divides up an input MR modality before pre-processing the intensity using a statistical normalization method. They had a 94% total accuracy rate.

By combining 2D and 3D MRI images, the authors of the study [20] offered a fusion strategy. They created DenseNet and 3D CNN architectures to categorize and segment multimodal images. The proposed technique worked superbly on the testing set, scoring 85% on certain 3D CNN models and 92% on DenseNet. Kang et al. [21] anticipated a technique for categorizing brain tumors with ML classifiers and a set of specific characteristics from deep-trained CNNs. Here, the author employed three diverse dataset sizes where a SVM classifier with radial basis function gives superior accuracy compared to other ML and DL classifiers. A fully automated prediction system based on ML was created in [22] to distinguish between images with high- and low-level glioma sickness. With 90% and 95% accuracy, the researchers classified tumors to primary, secondary and central nervous system tumors using an extreme gradient boosting model. A more successful classification and segmentation ensemble was suggested by the authors of [23] model using an approach combines the FCM clustering and deformable techniques." It was discovered through experimentation that the ensemble technique, which had a 95% classification accuracy rate, produced better outcomes.

Based on deep learning, Abiwinanda et al. [24] provided CNN algorithms to distinguish between benign and malignant brain tumor images. Numerous optimizers, such as RMSprop, Adam, and stochastic gradient descent, are used they solve the problems (SGD). According to their findings, a tailored AlexNet could excel at activities requiring medical imagery. A customized CNN architecture and VGGNet were created by the Meraj et al. [25] to classify 253 photographs of brain tumors, 155 of which were actual tumors and 98 of which were not. To decrease the overfitting of the suggested models, they used data preparation and augmentation approaches to increase the variety of the data samples. The customized VGGNet on a specific dataset displayed a maximum validation accuracy of 97%; the CNN model achieved validation accuracy of 85%. The classification results were greatly enhanced by the image pretreatment approaches evaluated by the authors of this work [26] for image editing. The authors suggested median blur, histogram equalization, Global thresholding, adaptive thresholding, the Sobel and high-pass filters, erosions and dilations, and global thresholding. A pre-trained Resnet101 V2 model built on transfer learning was also made available to help identify brain tumors in 3762 images. The accuracy of their conclusions was 95%. The researchers in this work [27] employed a hybrid approach using a genetic algorithm and CNNs (GA) to identify several forms of brain tumors, including glioblastoma. This suggested method automatically selected a CNN structure using a genetic process. The accuracy of the author's predictions for the three types of glioma images was 90.9%. Glioma, meningioma, and pituitary cancer were correctly classified in this study with a 94.2% accuracy rate.

A hybrid technique, known as VGGSCnet, was put forth by Ma et al. [28] by fusing VGGNet using several classifiers. Their research used a VGG-16 architecture that has already been trained to make training faster and more effective for autonomously detecting brain tumors from MRI data. The most prominent outlines of the region of interest were first selected through data pre-processing. The dataset's class imbalance problem was then resolved using the augmentation technique. Because the sixth layer offers fewer features, the features were extracted there. The presence of tumors in an image was determined using a stacked classifier. According to [29], an image of the anatomical structure is created via image pre-processing of the human body. MRI scans are utilized to find tumor cells in the sick person's brain. This research [30] proposes the 3D MRI brain tumor detection strategy that fuses multimodal information with CNN. To get the characteristics of brain tumor lesions under multiple modalities, multimodal 3D-CNNs were enhanced. The researchers gave a variety of CNN-based categorization algorithms, each with many repetitions, including VGGNets, GoogleNets, and ResNets. ResNet-

Doi : https://doi.org/10.54216/JCIM.140202
Received: January 19, 2024 Revised: March 01, 2024 Accepted: June 07, 2024

50 has a greater accuracy rate than VGGNets and GoogleNet achieving 96%, 93%, and 89%, respectively. Compared to VGGNet and GoogleNet, ResNet-50 offers 10% faster and 10% accurate findings.

3. Methodology

The suggested model investigates the layers and pre-trained algorithms in detail. Fig1 depicts the pre-processing, augmentations, training, and evaluation procedures for brain tumor images. The suggested deep learning (DL) algorithms employ several hyper-parameters for training and optimization; transfer learning and fine-tuning techniques are developed. An optimizer algorithm changes neural networks' biases and learning rates. Consequently, it aids in boosting accuracy while decreasing total loss. How well an algorithm matches the given data is demonstrated by a DL loss function. With an optimization function, the loss function learns to reduce the errorgradually.For this particular issue, the Adam optimizer and binary cross-entropy were utilized.

a. Dataset

This work considers brain T1-weighted CE-MR brain dataset collected from Nanfang hospital from 2005 to 2010 shown. It is composed of 3064 slices from 233 different patients. The slices are 512*512 pixels with 0.49 mm * 0.49 mm. These three diverse kinds of tumours are over there in the dataset, namely pituitary tumours, gliomas and meningiomas, as in Table 1. The three expert radiologists attain the pathology reports to know the pathology type and image labels. Here, the images are handled independently, where the radiologist can reach a consensus regarding the tumour label over every image. In this work, two tumour images of the same category are determined based on their relevance, i.e. similar and dissimilar.

Table 1: Brain image dataset summary

Category	Total patients	No. of slices	View	Total slices
Meningiomas	82	708	T	209
			S	231
			C	268
Gliomas	89	1426	T	494
			S	495
			C	437
Pituitary tumours	62	930	T	291
			S	320
			C	319

T- Transverse, S- Sagittal, and C- coronal

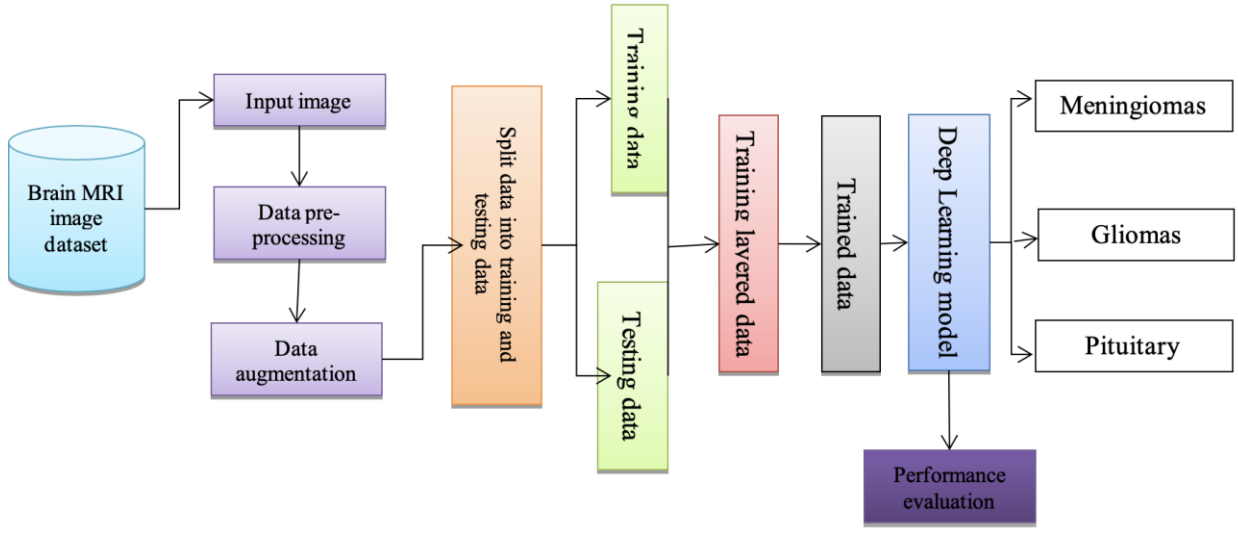

Figure 1: Block diagram of the proposed deep learning model

3.1. Pre-processing

MRI images are pre-processed before being fed into the algorithm. The first objective is optimizing the system by reducing the actual image size from $512 * 512 * 1$ to $128 * 128 * 1$pixels for easier computations and

Doi : https://doi.org/10.54216/JCIM.140202
Received: January 19, 2024 Revised: March 01, 2024 Accepted: June 07, 2024

demonstrating higher performance in lesser computation time. Data are segregated after being reorganized to prepare the unsorted data. Training, testing and validation data are produced following the division of the data into three parts (instance withlabeled target value). For testing and validation, 35% of the data are chosen, while 65% are used for training. The information is then improved so the model can identify it as essential information to increase the model's robustness and prevent over-fitting. The images have addeda gray-scale and noise distortion (augmentation). The augmentation technique enhances the actual images (by a factor of five). Image-based datasets are employed for grade categorization, and fifteen thousand three hundred seventeen photos make up the final dataset. Also, data augmentation is performed to generate newer data points.

3.2. Layered network model

The direction fields $L = (L_1, \dots, L_C)$ and the confidence maps$S = (S_1, S_2, \dots, S_J)$ is generated by the initial component. The symbols$S_j \in R^{w*h}, j \in \{1, \dots, J\}$ provide a 2D map that displays the degree of confidence that joint $j$as seen in the image. The 2D vector field encodes the orientation of the image $c$as $L_c \in R^{w*h*2}, c \in \{1, \dots, C\}$.

Fig 2 displays the network structure. Considering local data like small area around the image and long-range dependency association across brain regions, is crucial since the human pose is a typical structural prediction issues.A wider network's receptive field is crucial. The feature extractor is first used on image I to produce a feature map F that is used throughout all phases. The F resolution, as opposed to I, is decreased by 1/8 with this method. In step 1, F is used as an input for the confidence maps' regression S^1. Thanks to the 4×4 deconvolution with a stride equal to 2, the 1×1 convolution, in this instance, doubles the resolution of the output S^1 without requiring many more computations. After that, a separate sub-network formed by connecting F and $S^{1\prime}$ is used to regress the direction mappings L^1. (S down-sampled) to forecast S^t and L^t, we combine F, the input from stage t, the down-sampled output (S^{t-1} and L^{t-1}) and the output from the stage before. A 3-stage layered network can operate quickly and precisely, according to testing.

The confidence map makes it possible to determine the likelihood of seeing the MR images at different places. Consider a Gaussian peak where the image results in the optimum confidence map. Let $x^*_{j,k}$ be the tumor location coordinate and $S^*_{j,k}$ be the image confidence map for every individual$k$. As described, the confidence value at position p is:

$$S^*_{j,k}(p) = \exp\left(-\left|\left|p - x_{j,k}\right|\right|^2 / \sigma^2\right) \quad (1)$$

Where the Gaussian peak's spread is determined by σ. For an input image of the numerous input, the j confidence map is defined as:

$$S^*_j(p) = \max_k S^*_{j,k}(p) \quad (2)$$

The candidate maps are obtained during testing by applying non-maximum suppression on the confidence maps S.

Doi : https://doi.org/10.54216/JCIM.140202
Received: January 19, 2024 Revised: March 01, 2024 Accepted: June 07, 2024

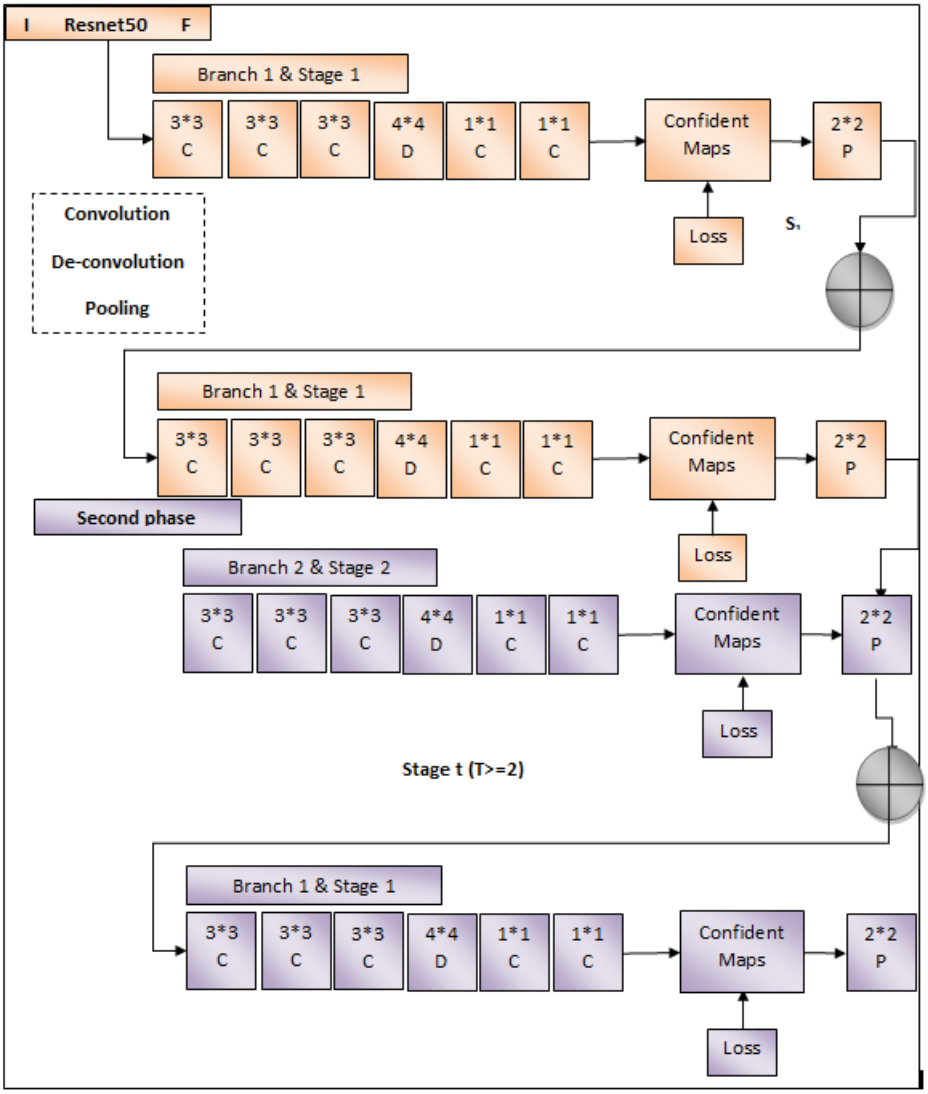

Figure 2: Layer details of network model

In Fig 2, networknodes connecting related features are provided.The connecting connections between the images are encoded in the direction fields. Each connection c of individual k corresponds to the direction field $L^*_{c,k}$, where 2D vector field encodes orientation and position data. The vector v produces the direction field as a rectangle with a width of two. The direction field $L^*_{c,k}$ at position p can then be found using the formula below:

$$L^*_{c,k} = \begin{cases} v & if\ p\ lies\ inside\ the\ 2\delta\ prediction\ region \\ 0 & else \end{cases} \quad (3)$$

Additionally, the unit vector in the direction of connection $cisv = (x_{j_{2,k}} - x_{j_{1,k}})/||x_{j_{2,k}} - x_{j_{1,k}}||$.Considering an input image including a large number of samples, the direction field of connection $c$is provided as follows:

$$L^*_c(p) = \frac{1}{n_c(p)} \sum_k L^*_{c,k}(p) \quad (4)$$

Here, the quantity of non-zero vectors at position p is known as $N_C(p)$. The candidate images are tested while they are connected using the direction field L. We assess the likelihood that any pair of joints, j_1 and j_2, will connect to pixels. The reference direction is denoted by the formula $d = x_{j2} - x_{j1}$, where x_{j1} and x_{j2} are the coordinates for j_1 and j_2, respectively. We produce a sample point set Q by randomly choosing a few locations along the line segment between j_1 and j_2. The comparison of the reference direction d and the direction's cosines field L_c is used to generate the confidence score for this link, and it is calculated as follows:

Doi : https://doi.org/10.54216/JCIM.140202
Received: January 19, 2024 Revised: March 01, 2024 Accepted: June 07, 2024

$$s(j_1, j_2) = \frac{1}{|Q|}\sum_{q \in Q} L_c(q).\ \frac{d}{||d||} \tag{5}$$

$|Q| \propto ||d||$ and $|Q|$ are the number of sampled points.We use supervision at every level to deal with this issue. We utilize the weighted loss function to prevent punishing true positive predictions. Additionally, the network is forced to converge to zero by a background prior. To contribute equally to the parameters update,we consider the gradient reactions between theforeground and backgroundconfidence maps. The loss at stage t is described as follows:

$$Loss_S^t = \sum_j \sum_p W(p).\ \left\|S_j^t(p) - S_j^*(p)\right\|^2 + \lambda \sum_p \left\|S_B^t(p) - S_B^*(p)\right\|^2 \tag{6}$$

$$Loss_L^t = \sum_c \sum_p W(p).\ ||L_c^t(p) - L_c^*(p)||^2 \tag{7}$$

Where S represents background and S_j^* refers ground-truth confidence map. L_c^* is the $c's$ ground-truth direction field. If point p is not annotated, the binary mask $W(p)$has the value of 0. To account for the loss from foreground and background, set $\lambda = 0.05$ with the complete loss felt at every stage.

3.3. Layered convolutional network model

The multi-layered convolutional network performance is limited because it was trained on still images in Fig 3. The consistency problem causes some noticeable errors in images. For real-time applications, it would be computationally expensive due to its multi-layered design and sophisticated architecture. For processing images, the lightweight model is preferred. Our bottom-up instance estimate method was built on the LSTM model for a single sample which we expanded to handle several samples. We use the network in Fig 3 in a neural network by applying the weight-sharing approach to the various network stages. The following image frames are input at various locations around the network. We additionally employ the LSTM units in the intervals between the frames to construct an LSTM with more memory.

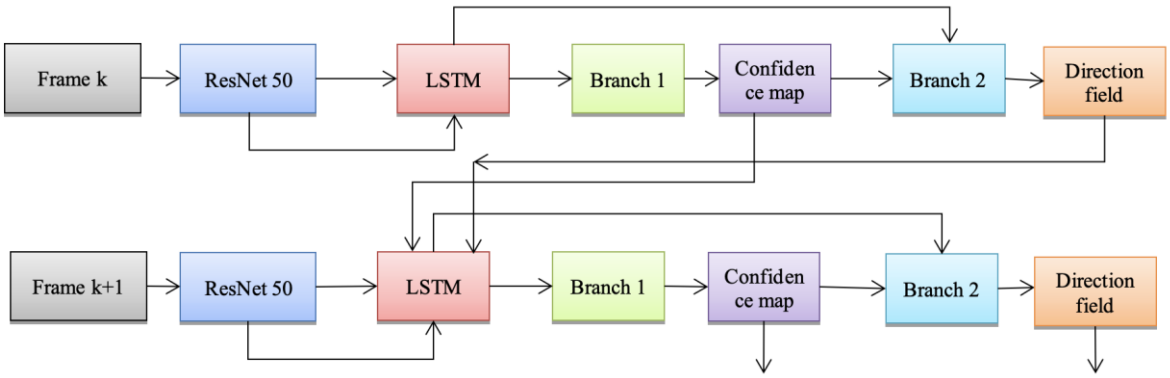

Figure 3: Layered LSTM model

The LSTM pose machine network must identify the confidence maps for every frame. The direction fields and confidence maps can accommodate many samples and create a two-branch network topology to account for each. Our network structure for estimating multiple image frames. There are two branches and several stages in the network. The direction fields and confidence maps predict the frames for each stage's examination of a single frame. ResNet50 algorithm is utilized to haul out the image attributes of the present frame. The preceding image pose is employed. LSTM module then provides the concatenated image characteristics and the previous frame's forecast outcomes. Then, $Branch1$ and $Branch2$ will forecast the reliability maps and direction values for the current frame using the output from the LSTM. Despite having different topologies, $Branch1$ and $Branch2$ share weight with their equivalent stages $t \geq 2$. Since the initial frame has no preceding frames, it is an exception. To get the first frame's direction fields and confidence maps to send it to the LSTM module, utilize the branches (two) of the initial stage. The model is used to forecast the variable length image. It not only predicts the tumor, but it

Doi : https://doi.org/10.54216/JCIM.140202
Received: January 19, 2024 Revised: March 01, 2024 Accepted: June 07, 2024

also significantly cuts runtime and parameter requirements. The network allows estimating image locations from an image of varying length. In addition to predicting cancer occurrence, it drastically decreases the parameters and runtime.

3.4. Long Short-Term Memory

LSTM offers steady and precise results for tumor predictions while capturing image consistency. This work uses the LSTM with the layered model. The conventional LSTM with input, output and forget gates have given higher performance when evaluated to other LSTM variations. The spatial information of the frames must be preserved; LSTM module employs 2D maps as the input indeed of 1D vectors. The default LSTM unit changes as follows based on the input feature mappings X_t at time step t:

$$I_t = \sigma(W_{xi} * X_t + W_{hi} * H_{t-1} + b_i) \quad (8)$$
$$F_t = \sigma(W_{xf} * X_t + W_{hf} * H_{t-1} + b_f) \quad (9)$$
$$O_t = \sigma(W_{xo} * X_t + W_{ho} * H_{t-1} + b_o) \quad (10)$$
$$\tilde{C}_t = \tanh(W_{xc} * X_t + W_{hc} * H_{t-1} + b_c) \quad (11)$$
$$C_t = F_t \odot C_{t-1} + I_t \odot \tilde{C}_t \quad (12)$$
$$H_t = O_t \odot \tanh(C_t) \quad (13)$$

Where $*$ signifies the element-wise product and means the convolution operation. Here,$W_{x\sim}$ and $W_{h\sim}$ 2D convolutional kernels. The spatial dimensions are all preserved in the tensors of the gates I_t, F_t, O_t the memory cell C_t, C_{t-1} the candidate memory $\tilde{C}_t$ and the hidden state $H_t\ and\ H_{t-1}$.Consecutive frames from the training sequence are fed into the cascaded layered stages, where each stage receives one frame as input. At each frame, true data probability maps and direction fields are provided. To continuously monitor the training, the loss for the direction fields and confidence maps will be added at each level. Training must reduce the overall $l_2$for all input frames, separating the prediction and the groundtruth. The ground truth for the various stages is taken from the relevant frames, although the loss term is defined similarly in Eq. (14).

$$Loss_L^t = \sum_c \sum_P W(p).\left|\left|L_c^t(p) - L_c^*(p)\right|\right|^2 \quad (14)$$

Here, L_c^* represents ground truth direction with connection c. W is binary mask with $W(p) = 0\ (no\ annotation)$.The input image is randomly rotated with a degree in $[-30^0, 30^0]$ and horizontally flipped to increase the training data for the image posture machine. We use the MATLAB framework to apply our methodology. The weights have been pre-trained to initialize the feature extractor module (ResNet50). The Adam solution trains the entire network with a batch size of 16. The work employs a starting learning rate of $8 * 10^{-5}$. Each input image is examined at three different scales before the output direction fields, and confidence maps are averaged across the scales $(0.7, 1.0, and\ 1.3)$.We maintain the feature extractor modules weight in the image trained with the LSTM. Our model's length is five, which displays sufficient data to detect major alterations in an image series.

4. Numerical results

The open-access dataset was used to test the suggested model. The MATLAB 2020a implementation of the optimized layered network model was built on top of the frameworks. The entire network was trained on the PC with a configurationof2.60 GHz Intel Core i5-11400 processor. After the initial layers of the fundamental model were frozen, the network model was first imported. The entire network was fine-tuned in the second phase and retrained using the brain tumor MR images and our recommended ending layers. We also compared the suggested layered network model with other CNN models to verify our experiment.

4.1. Evaluation metrics

A common tool for assessing the confusion matrix indicates how effectively trained model may forecast data from a particular dataset for verification. The ground truth labels and the actual class are displayed in equivalent rows and columns (i.e., tumors or non-tumors). For each validation sample, the predicted statistics show the percentage of accurate and false classifications. A true positive is equal to the number of samples that were correctly identified as positive. On the contrary, a true negative equal the number of samples predicted correctly as negative. The prediction was mistakenly labeled as favorable when they weren't known as false positives. False negatives are negative outcomes that appear positive. The effectiveness of the anticipated model is assessed with wider range

Doi : https://doi.org/10.54216/JCIM.140202
Received: January 19, 2024 Revised: March 01, 2024 Accepted: June 07, 2024

of parameters like validation accuracy, recall, precision, F1 score and Receiver operating characteristic (ROC) curve. F1-score, recall, accuracy and precision of each model were calculated using the following formulas:

$$Precision = \frac{TP}{TP + FP} \quad (15)$$

$$Sensitivity = \frac{TP}{TP + FN} \quad (16)$$

$$Specificity = \frac{TN}{TN + FP} \quad (17)$$

$$Accuracy = \frac{TP + TN}{TP + TN + FP + FN} \quad (18)$$

$$F1 - score = \frac{2(TP)}{2(TP) + FP + FN} \quad (19)$$

4.2. Analysis

MR images were obtained from open access on Kaggle; the suggested layered model was trained with parameter adjustments. Results from training and validation are covered in this section. The size and quality of this particular dataset were improved using several pre-processing and data augmentation approaches. We trained our proposed model with a range of hyper-parameters for improved training. We employed the Adam optimizer with batch processing and cross-entropy loss function with a minimal learning rate of $10e^{-5}$and an initial learning rate of $10e^{-3}$. Our favored classifier was sigmoid. During this period, we trained our optimized architecture utilizing the backend process. The suggested model was trained using training data 80% of the time and validation 20% of the time. The results of the validation and training are represented in Fig 11. The loss curves with training epochs are depicted in Fig 12. The graph of the anticipated model shows that, for the specified hyper-parameters, the training and validation sets' accuracy increased rapidly with the number of epochs until it stabilized. Using the assessment above measures, the proposed model was utilized to quantify the proposed model performance and count the amount of data that was accurately and successfully classified. The proposed model's assessment metric score is shown in Fig 9.

ROC curve in Fig 8where the model illustrates the brain tumor detection model performs. For several classifiers, the area under the curve (AUC), representing the degree of differentiation between classes, is an important evaluation measure. It shows how well the model distinguishes across categories. The model's ability to identify between patients who suffer from the illness and those who do not improve with increasing AUC.AUC values close to 1 on an efficient model indicate a high level of competency. As can be seen, the layered model demonstrated an AUC score of 99%. Fig 4 shows how the suggested strategy successfully recognized the brain MR images. When a tumor is absent, the model considers that the image is simply typical $(True: 0)$. Still, it predicts that it is present when one is present $(Pred: 1)$ and $(Pred: 0)$.The suggested approach incorrectly identifies the brain MRI images, as seen in Fig 4. The model implies a tumor is absent if the image contains $(True: 1)$ $(Pred: 0)$. The model entails it has a tumor if it does not $(True: 0)$ $(Pred: 1)$.

4.3. Comparative analysis

Some CNN architectures were compared in this work, including VGG16, GoogLeNet, InceptionResNetV2, Xception, ResNet50 and EfficientNet-B0. Fig 5 to Fig 8 shows the anticipated model's evaluation measure score. The proposed model's ROC plot is depicted in Fig 8. In each investigation, CNN used the same characteristics and attributes that vary with the FC and convolution layer thickness. The validation accuracy for the improved network and other DL approaches were previously trained and used in this experiment is displayed in Table 1 for comparison. The other computed evaluation measures are also shown. Every model, except InceptionResNetV2, initially shows an over-fitting issue and displays a minimum error gap after each phase. Every other model displayed a highly consistent loss minimization.

Table 2: Comparison of various performance metrics

Methods	Accuracy (%)	Precision (%)	Recall (%)	F-measure (%)	ROC	Error rate	MCC
Hybrid CNN and NADE	95%	94.49	94.64	94.56	0.86	0.089	0.4656
CNN	96.13%	95.61	95.62	95.46	0.855	1.02	0.4534
CNN and KELM	93.6%	83.4	76.5	72	0.84	1.56	0.4317

Doi : https://doi.org/10.54216/JCIM.140202
Received: January 19, 2024 Revised: March 01, 2024 Accepted: June 07, 2024

Deep CNN with data augmentation	94.58%	81.2	75	77.9	0.80	1.63	0.4658
CNN and Genetic Algorithm	94.2%	91.97	96.62	94.24	0.78	0.077	0.4205
Hybrid VGG16-NADE	96.01%	95.72	95.64	95.68	0.91	0.075	0.3564
ResNet+SE	98.8%	99.5	99.15	99.10	0.98	0.065	0.2645
Layered Network model (proposed)	99.05%	**100%**	**100%**	**99.5%**	**0.99**	0.055	**0.1253**

Table 2 compares various metrics like prediction accuracy, recall, precision, F-measure, ROC, error rate and MCC. The prediction accuracy of the layered network model is 99% which is 4%, 2.87%,5.4%,4.42%, 4.24%, 4.63%,2.99% and 0.2% higher than hybrid CNN and NADE, CNN, CNN and KELM, deep CNN with data augmentation, CNN-GA, hybrid VGG16-NADE and ResNet+SE. The precision of layered network is 100% which is 5.51%, 4.39%, 16.15%, 18.35%, 7.58%, 4.28% and 0.5% higher than hybrid CNN and NADE, CNN, CNN and KELM, deep CNN with data augmentation, CNN-GA, hybrid VGG16-NADE and ResNet+SE. The recall of the layered network model is 100% which is 5.36%, 5.38%, 23.5%, 25%, 3.38%, 4.36% and 0.85% higher than hybrid CNN and NADE, CNN, CNN and KELM, deep CNN with data augmentation, CNN-GA and hybrid VGG16-NADE. The F-measure of the layered network model is 99.5% which is 4.94%, 4.04%, 27.5%, 21.6%, 5.25%,3.85% and 0.40% higher than hybrid CNN and NADE, CNN, CNN and KELM, deep CNN with data augmentation, CNN-GA, hybrid VGG16-NADE and ResNet+SE model. The ROC of the proposed layered network mode is comparatively higher than other approaches, i.e., 0.12, 0.125, 0.14, 0.18, 0.2 and 0.07, more elevated than different approaches. The error rate of the proposed model is 0.055, which is lesser than other approaches. Generally, the MCC value should range from -1 to 1; however, the proposed model gives a better MCC value of 0.1253 while the others are 0.4656, 0.4534, 0.4317, 0.4658, 0.4205, 0.3564 and 0.2645respectively (See Fig 4 to Fig 9).

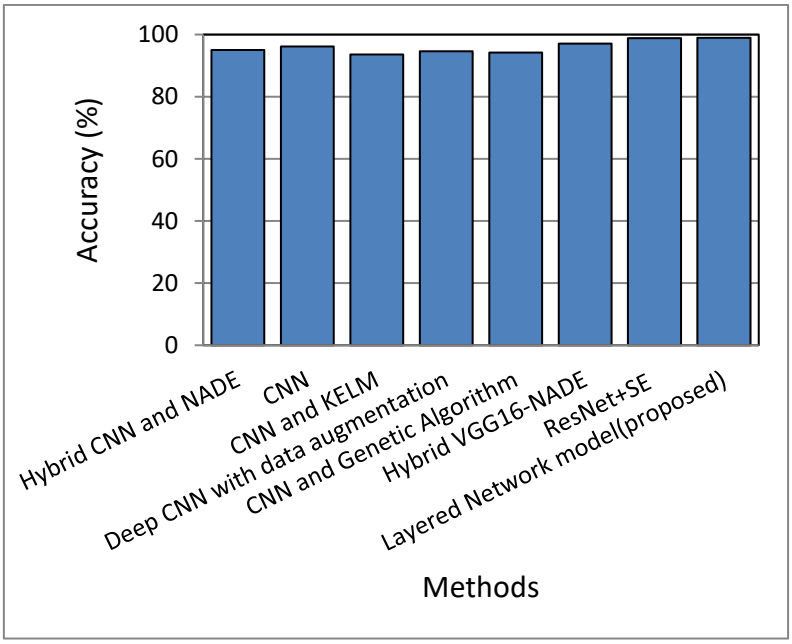

Figure 4: Accuracy comparison

Doi : https://doi.org/10.54216/JCIM.140202
Received: January 19, 2024 Revised: March 01, 2024 Accepted: June 07, 2024

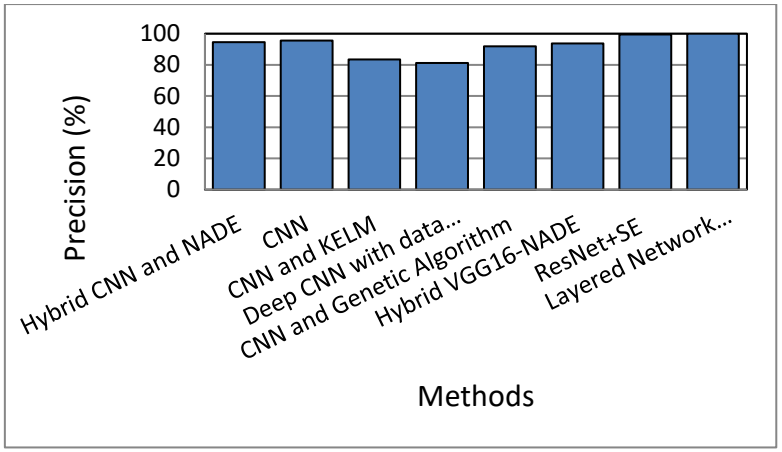

Figure 5: Precision comparison

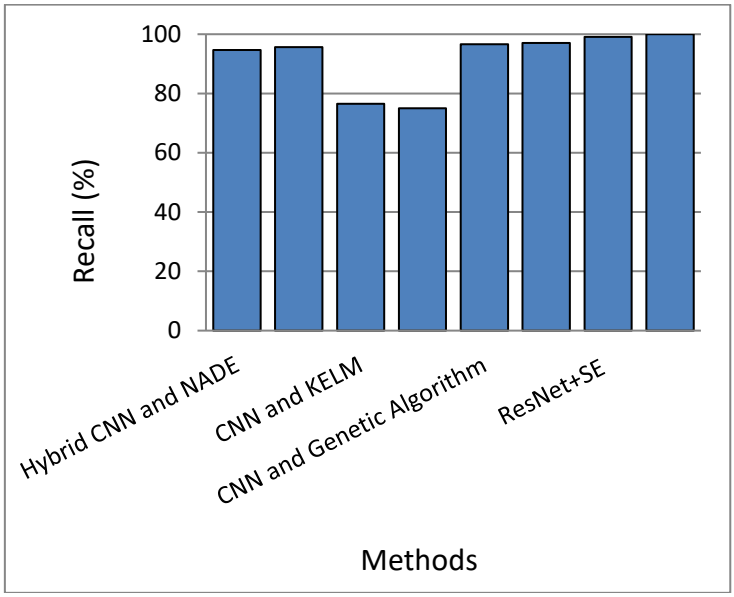

Figure 6: Recall comparison

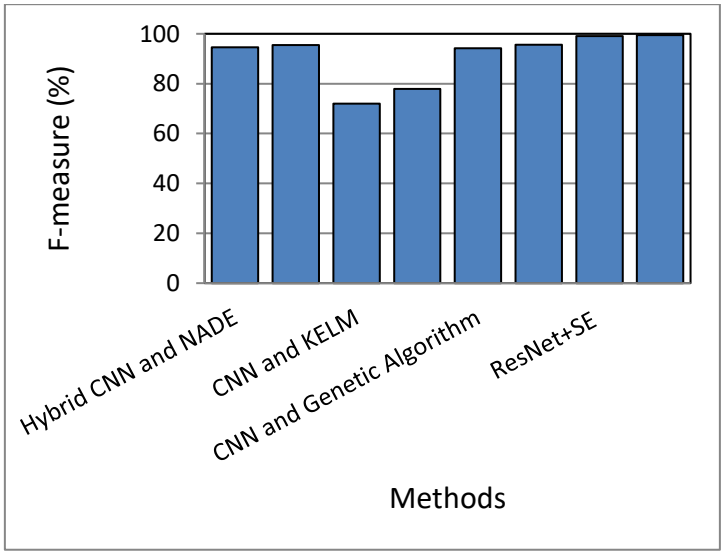

Figure 7: F-measure comparison

Doi : https://doi.org/10.54216/JCIM.140202
Received: January 19, 2024 Revised: March 01, 2024 Accepted: June 07, 2024

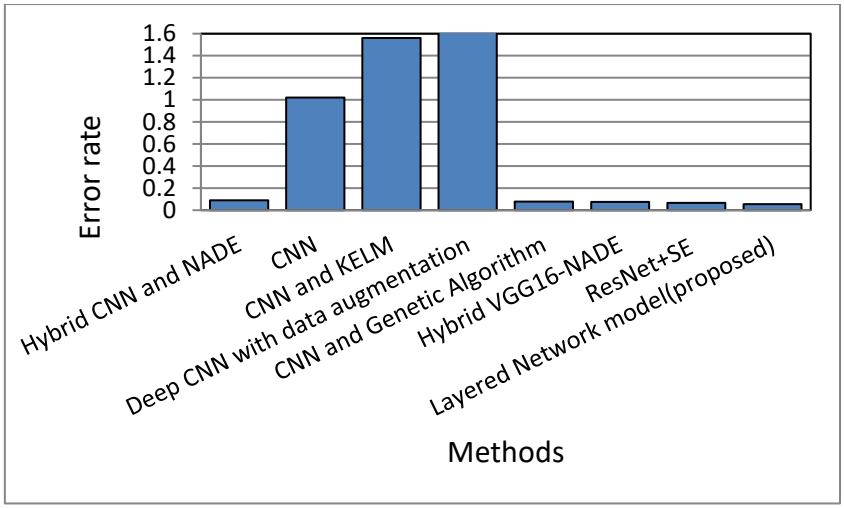

Figure 8: Error rate comparison

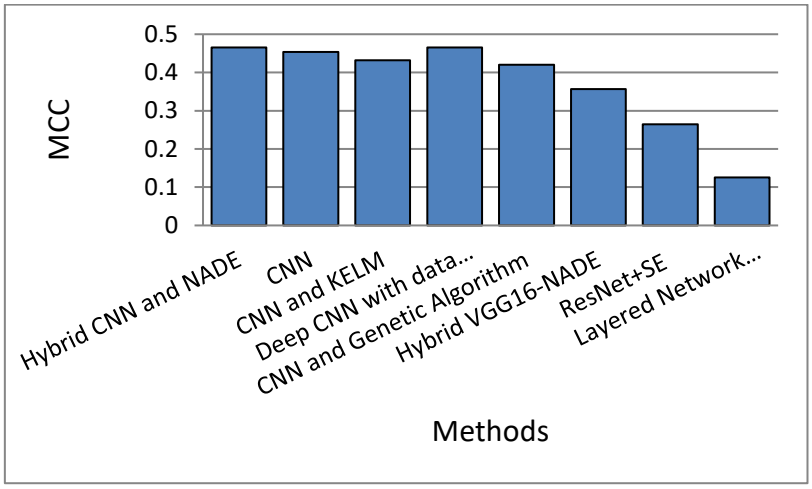

Figure 9: MCC comparison

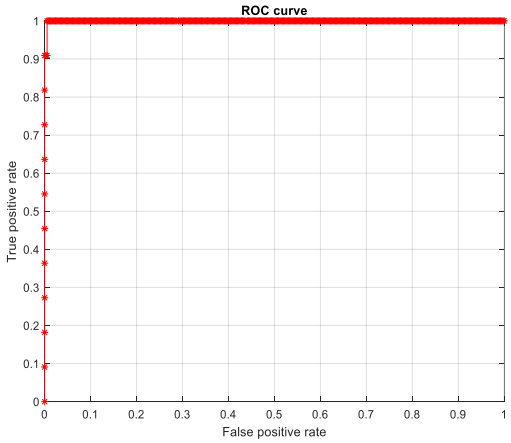

Figure 10: ROC curve

Doi : https://doi.org/10.54216/JCIM.140202
Received: January 19, 2024 Revised: March 01, 2024 Accepted: June 07, 2024

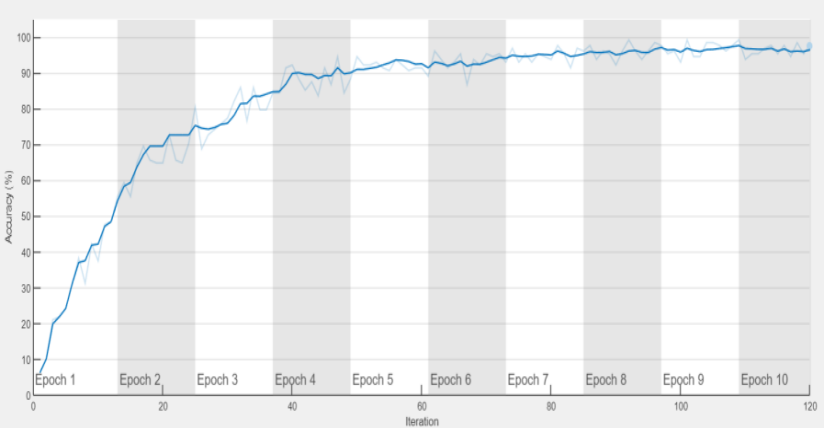

Figure 11: Accuracy computation

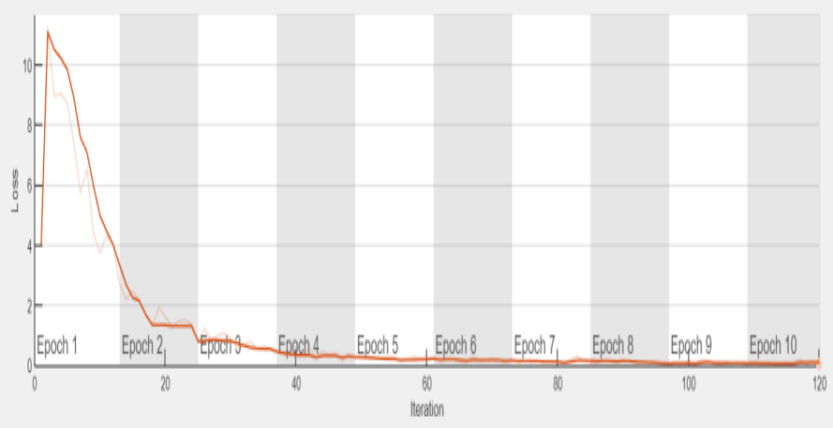

Figure 12: Loss computation

The existing study investigated the transfer learning strategy for identifying brain cancers in MR images using the deep network using the layers. Compared to the other networks indicated below, the suggested improved network performance was achieved, with the validation data being accurate to the highest possible degree (99%).Subsequently, VGG16 model was used to test the transfer learning method for identifying brain tumors. On the validation data, the improved VGG16 network obtained 98.64% accuracy. InceptionV3 was utilized to examine the effectiveness of the brain tumor prediction based on transfer learning. It achieved 97% validation accuracy. Xception demonstrated the model's effectiveness by reaching a total validation accuracy of 97.8%. On validation data, the InceptionResNetV2 algorithm obtained 98% accuracy. Additionally, the pre-trained version of ResNet50 was utilized to identify brain cancers in MR images. The ResNet50 algorithm's results revealed the lowest average of 95.8% of the tested models in this study had precision on the test dataset. The comparison and analysis of the outcomes of each structure using the new approach. The recommended model achieved maximum accuracy by using more images of brain tumors than the CNN methods. Table 1 provides a performance assessment of the ML and DL-based techniques used in this investigation to identify brain tumors. The variations in data preparation, learning and validation methods show how much computer power is employed in each approach. The following papers are not directly compared in this research. The proposed model, however, achieved 98.87% total accuracy, which we found to be exceptional in terms of accuracy. The quantity, dimensions, and weight of the several fine-tuned CNNs used in this investigation are covered. The proposed fine-tuned layered model poses distinct parameters and the shortest size of only 16.8 MB. It is one of the smallest and most efficient models. Because of this, the weight size of the VGG16 model is 56MB, with 17,092 parameters, as opposed to 83MB and 28,356 parameters for the InceptionV3 model. The following Xception result has 33,096 total parameters and a weight size of 87MB.ResNet50 features 36,410 total parameters and a total weight size of 93MB, which is larger than the preceding iterations, with InceptionResNetV2 having the largest weight size of 210MB.

5. Conclusion

Due to the growing need for the effective and precise analysis of enormous volumes of medical data, MR imaging for diagnosing brain tumors has become increasingly popular. Brain tumors are fatal; manual detection takes time and relies on medical competence. It will be necessary to use an automatic diagnostic method to find anomalies

Doi : https://doi.org/10.54216/JCIM.140202
Received: January 19, 2024 Revised: March 01, 2024 Accepted: June 07, 2024

in MRI. Therefore, this work created an effective, layered network model-based architecture to predict brain tumors from MRI. With a prediction accuracy of 99%, the suggested technique demonstrated the highest performance in identifying brain tumors. In medical imaging, this work focused on the convolutional models for brain tumors; more study is required. This work considers more powerful and substantial deep-layered models in the future to categorize and segment brain tumors with less time complexity. We will also add more MRI images to the dataset used in this investigation to improve the suggested model's accuracy. To lay the foundation for upcoming work, we will extend the suggested methodology to additional medical images like computed tomography (CT), x-ray and ultrasound.

References

[1] F. Islami, C. E. Guerra, A. Minihan, K. R. Yabroff, ‘‘American Cancer Society’s report on the status of cancer disparities in the United States, 2021,’’ CA, Cancer J. Clinicians, vol. 72, no. 2, pp. 112–143, Mar. 2022.

[2] Saeed, A. Paul, P. Karthigaikumar, and A. Nayyar, ‘‘Convolutional neural network based early fire detection,’’ Multimedia Tools Appl., vol. 79, nos. 13–14, pp. 9083–9099, Apr. 2020.

[3] F. Saeed, A. Paul, W. H. Hong, and H. Seo, ‘‘Machine learning based approach for multimedia surveillance during fire emergencies,’’ Multimedia Tools Appl., vol. 79, nos. 23–24, pp. 16201–16217, Jun

[4] He, X. Zhang, S. Ren, and J. Sun, ‘‘Deep residual learning for image recognition,’’ in Proc. IEEE Conf. Comput. Vis. Pattern Recognit. (CPR), Jun. 2016, pp. 770–778.

[5] Abd-Ellah, A. I. Awad, A. A. M. Khalaf, and H. F. A. Hamed, ‘‘Two-phase multi-model automatic brain tumor diagnosis system from magnetic resonance images using convolutional neural networks,’’ Eurasip J. Image Video Process., vol. 2018, p. 97, Dec. 2018.

[6] Somasundaram and R. Gobinath, ‘‘Current trends on deep learning models for brain tumor segmentation and detection—A review,’’ in Proc. Int. Conf. Mach. Learn., Big Data, Cloud Parallel Comput. (COMITCon), Feb. 2019, pp. 217–221.

[7] Kumar, P. Kumar, and D. Kumar, ‘‘Brain tumor detection using convolutional neural network,’’ in Proc. IEEE Int. Conf. Mobile Netw. Wireless Commun. (ICMNWC), Dec. 2021, pp. 1–6.

[8] Kang, Z. Ullah, and J. Gwak, ‘‘MRI-based brain tumor classification using ensemble of deep features and machine learning classifiers,’’ Sensors, vol. 21, no. 6, p. 2222, Mar. 2021

[9] H. Yahyaoui, F. Ghazouani, and I. R. Farah, ‘‘Deep learning guided by an ontology for medical images classification using a multimodal fusion,’’ in Proc. Int. Congr. Adv. Technol. Eng. (ICOTEN), Jul. 2021, pp. 1–6.

[10] K. R. Bhatele and S. S. Bhadauria, ‘‘Machine learning application in glioma classification: Review and comparison analysis,’’ Arch. Comput. Methods Eng., vol. 29, pp. 247–274, Apr. 2021

[11] Mehrotra, M. A. Ansari, R. Agrawal, and R. S. Anand, ‘‘A transfer learning approach for AI-based classification of brain tumors,’’ Mach. Learn. with Appl., vol. 2, Dec. 2020, Art. no. 100003.

[12] Methil, ‘‘Brain tumor detection using deep learning and image processing,’’ in Proc. Int. Conf. Artif. Intell. Smart Syst. (ICAIS), Mar. 2021, pp. 100–108.

[13] Najib, M. M. Rahman, T. M. S. Sazzad, N. I. Khan, and S. K. Dey, ‘‘VGG-SCNet: A VGG net-based deep learning framework for brain tumor detection on MRI images,’’ IEEE Access, vol. 9, pp. 116942–116952, 2021

[14] Li, L. Kuang, S. Xu, and Z. Sha, ‘‘Brain tumor detection based on multimodal information fusion and convolutional neural network,’’ IEEE Access, vol. 7, pp. 180134–180146, 2019.

[15] Siddique, S. Sakib, M. M. R. Khan, A. K. Tanzeem, M. Chowdhury, and N. Yasmin, ‘‘Deep convolutional neural networks model-based brain tumor detection in brain MRI images,’’ in Proc. 4th Int. Conf. I-SMAC (IoT Social, Mobile, Anal. Cloud) (I-SMAC), Oct. 2020, pp. 909–914.

[16] Sangeetha, A. Mohanarathinam, G. Aravindh, S. Jayachitra, and M. Bhuvaneswari, ‘‘Automatic detection of brain tumor using deep learning algorithms,’’ in Proc. 4th Int. Conf. Electron., Commun. Aerosp. Technol. (ICECA), Nov. 2020, pp. 1–4.

[17] Chollet, ‘‘Xception: Deep learning with depthwise separable convolutions,’’ in Proc. IEEE Conf. Comput. Vis. Pattern Recognit. (CPR), Jul. 2017, pp. 1800–1807.

[18] Russakovsky, J. Deng, H. Su, J. Krause, S. Satheesh, S. Ma, Z. Huang, A. Karpathy, A. Khosla, and M. Bernstein, ‘‘ImageNet large scale visual recognition challenge,’’ Int. J. Comput. Vis., vol. 115, no. 3, pp. 211–252, Dec. 2015.

[19] Dogo, O. J. Afolabi, N. I. Nwulu, B. Twala, and C. O. Aigbavboa, ‘‘A comparative analysis of gradient descent-based optimization algorithms on convolutional neural networks,’’ in Proc. Int. Conf. Comput. Techn., Electron. Mech. Syst. (CTEMS), Dec. 2018, pp. 92–99.

Doi : https://doi.org/10.54216/JCIM.140202
Received: January 19, 2024 Revised: March 01, 2024 Accepted: June 07, 2024

[20] Q. Wei and L. R. Dunbrack, ‘‘The role of balanced training and testing data sets for binary classifiers in bioinformatics,’’ PLoS ONE, vol. 8, pp. 1–12, Jul. 2013.
[21] B. H. Menze, A. Jakab, S. Bauer, J. Kalpathy-Cramer, K. Farahani, J. Kirby, Y. Burren, N. Porz, J. Slotboom, and R. Wiest, ‘‘The multimodal brain tumor image segmentation benchmark (BRATS),’’ IEEE Trans. Med. Imag., vol. 34, no. 10, pp. 1993–2024, Oct. 2015.
[22] Q. Wen, L. Sun, F. Yang, X. Song, J. Gao, X. Wang, and H. Xu, ‘‘Time series data augmentation for deep learning: A survey,’’ 2020, arXiv:2002.12478.
[23] Razzak, M. Imran, and G. Xu, ‘‘Efficient brain tumor segmentation with multiscale two-pathway-group conventional neural networks,’’ IEEE J. Biomed. Health Information., vol. 23, no. 5, pp. 1911–1919, Sep. 2019.
[24] Abiwinanda, M. Hanif, S. T. Hesaputra, A. Handayani, and T. R. Mengko, ‘‘Brain tumor classification using convolutional neural network,’’ in World Congress on Medical Physics and Biomedical Engineering. Bhopal, India: Springer, 2019, pp. 183–189.
[25] Meraj, A. Hassan, S. Zahoor, H. T. Rauf, M. I. Lali, L. Ali, and S. A. C. Bukhari, ‘‘Lungs nodule detection using semantic segmentation and classification with optimal features,’’ Neural Comput. Appl., vol. 33, no. 17, pp. 10737–10750, 2019
[26] Hossain, F. Shishir, and M. Ashraf, ‘‘Brain tumor detection using CNN,’’ Turkish J. Comput. Math. Educ., vol. 12, no. 11, pp. 4597–4603, 2021.
[27] Piyush K. Pareek, Pixel Level Image Fusion in Moving objection Detection and Tracking with Machine Learning “,Fusion: Practice and Applications, Volume 2 , Issue 1 , PP: 42-60, 2020
[28] Shivam Grover, Kshitij Sidana, Vanita Jain, “Egocentric Performance Capture: A Review”, Fusion: Practice and Applications, Volume 2, Issue 2 , PP: 64-73, 2020.
[29] Abdel Nasser H. Zaied, Mahmoud Ismail and Salwa El- Sayed, A Survey on Meta-heuristic Algorithms for Global Optimization Problems, Journal of Intelligent Systems and Internet of Things,Volume 1 , Issue 1 , PP: 48-60, 2020
[30] Mahmoud H.Alnamoly, Ahmed M. Alzohairy, Ibrahim M. El-Henawy, “A survey on gel images analysis software tools, Journal of Intelligent Systems and Internet of Things,Volume 1 , Issue 1 , PP: 40-47, 2021.

Doi : https://doi.org/10.54216/JCIM.140202
Received: January 19, 2024 Revised: March 01, 2024 Accepted: June 07, 2024